# Structural, magnetic, electronic, and spin transport properties of epitaxial $Fe_3Si/GaAs(001)$

A. Ionescu, C. A. F. Vaz, T. Trypiniotis, C. M. Gürtler, H. García-Miquel,* and J. A. C. Bland†
*Cavendish Laboratory, University of Cambridge, Madingley Road, Cambridge, CB3 0HE, United Kingdom*

M. E. Vickers
*Department of Materials Science and Metallurgy, University of Cambridge, Pembroke Street, Cambridge, CB2 3QZ, United Kingdom*

R. M. Dalgliesh and S. Langridge
*Rutherford-Appleton Laboratory, Chilton, OX11 0QX, United Kingdom*

Y. Bugoslavsky, Y. Miyoshi, and L. F. Cohen
*Blackett Laboratory, Imperial College, London, SW7 2BW, United Kingdom*

K. R. A. Ziebeck
*Department of Physics, University of Loughborough, Loughborough, LE11 3TU, United Kingdom*
(Received 10 September 2004; published 1 March 2005)

We report experimental results on the structural, magnetic, electronic, and spin transport properties of a 21 nm $Fe_3Si/GaAs(001)$ heterostructure epitaxially grown by coevaporation. High-resolution x-ray diffraction shows an almost stoichiometric film, which is lattice matched in-plane to the GaAs substrate and therefore slightly tetragonal distorted. Polarized neutron reflectometry measurements yield a magnetic moment of $(1.107\pm0.014)\mu_B$ per atom at room temperature (RT), while superconducting quantum interference device magnetometry yields a magnetic moment of $(0.9\pm0.1)\mu_B$ per atom at RT, both close to the bulk value. Magneto-optic Kerr effect measurements show that this system has in-plane cubic anisotropy with easy axes along the $\langle 100\rangle$ directions and a cubic anisotropy constant $K_1=(3.1\pm0.6)\times10^4$ erg/cm$^3$ at RT. A resistivity of $(4.1\pm0.4)\times10^{-7}$ Ω m in the $Fe_3Si$ film was measured, which is close to the bulk value. Optical spin orientation in the GaAs was used for spin transport measurements and spin detection is demonstrated at RT for this system. Point contact Andreev reflection spectroscopy was used to determine the spin polarization of the transport current, yielding $P=(45\pm5)\%$.

DOI: 10.1103/PhysRevB.71.094401 PACS number(s): 75.70.Ak, 72.25.Mk, 68.55.Jk, 75.60.Ej

## I. INTRODUCTION

Heusler alloys[1] in thin film form are currently attracting much interest due to their potential for applications in future magnetoelectronic and spintronic devices, e.g., as possible spin injector electrodes in tunnel magnetoresistance structures,[2,3] in spin valves to increase the giant magnetoresistance effect,[4] or for spin polarized current injection into semiconductors. The main interest in these compounds arises from the fact that the "half" Heusler alloys ( *XYZ*, where *X* and *Y* are transition metals and *Z* is a *B* subgroup element, e.g., NiMnSb) are predicted by band structure calculations to be half-metallic ferromagnets (HMF's) due to the asymmetric band profile reflected in the character of the $C1_b$ structure in which they crystallize.[5,6] Half-metallic (HM) means that the minority-spin electrons are semiconducting, whereas the majority-spin electrons are metallic at the Fermi level. Consequently, these materials should be 100% spin polarized at 0 K. For the full Heusler alloys ($X_2YZ$) crystallizing in the $L2_1$ structure, some exhibit a state close to a HMF with a deep "pseudogap"[5,6] [minority-spin density of states (DOS) close to zero at the Fermi level], for instance $Co_2MnZ$, where $Z=$Al, Sn,[7] Si, and Ge.[8] More recent band structure calculations by Ishida *et al.*[9] extend the work on the $C1_b$ structure and postulate also other "half" Heusler alloys to be HM under certain conditions, such as reduced lattice parameters due to external pressure or special atomic configurations. Furthermore, Fujii *et al.*[10] postulate that some $L2_1$ structure type (full Heusler alloys) are HM, as for the case of ferromagnetic $Fe_2MnSi$ with a real gap in the DOS of the minority band. In the last few years $Co_2MnSi$ has been widely investigated experimentally in thin film form,[3,11–15] because of its high Curie temperature $T_C=985$ K (the highest among all known Heusler alloys containing Mn[16] ). In addition, new DOS calculations of Ishida *et al.*[17] attest a real minority-spin gap of $\approx$0.42 eV in the bulk case, while indicating also that for films HM behavior depends on thickness and surface termination as well as surface orientation, (111) being better than (001) films to obtain HM behavior.[18] As is already known for some bulk Heusler alloys[19] as well as for films,[4] antisite disorder between Co and Mn (Refs. 11–13) (e.g., indicated by a high electrical resistivity as compared to bulk) particularly at the surface, changes the termination of the film and destroys the HM behavior, therefore reducing the amount of spin polarization.[18,20] In addition, due to their ternary nature, Heusler alloy stoichiometries in thin films are difficult to control leading easily to excess or deficiency of one atom species[12,13] and to deviations in the expected physical properties.[12,15] Moreover, the existence of nonferromagnetic interfaces as reported by Geiersbach *et al.*,[13] which are present in their Co-based Heusler alloys films, are detrimental for spin injection. The measured transport spin polariza-

 

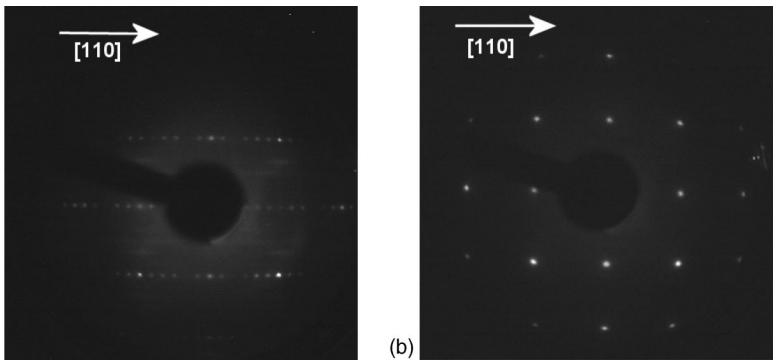


FIG. 1. (a) LEED image of a "pseudo" ($P4\times6$) reconstructed GaAs(001) surface prior to growth; $E=125$ eV. (b) Image of a 74 ML(21 nm) thick $Fe_3Si$ film showing that the cubic $L2_1$ ("Heusler") structure has been stabilized; $E=115$ eV.

tion of some Heusler alloy films has been disappointingly low at $P=58\%$(NiMnSb, Ref. 21) and $P=54\%$($Co_2MnSi$, Ref. 14) at 4.2 K as measured by point contact Andreev reflection. The reason for this reduced spin polarization might be due to a combination of the above factors, namely, surface termination and orientation, structural inhomogeneities, and nonmagnetic interfaces, and/or, as recently argued by Dowben and Skomski, due to some fundamental restrictions of true HM behavior in perfect crystals at 0 K.[22] These authors show that magnon and phonon excitations reduce the spin polarization at finite temperatures and suggest that elementary ferromagnets (Fe, Co, Ni) are better candidates for spin injection than HM systems. However, for spin injection into semiconductors (SC's) these ferromagnetic metals (FM's) and their alloys have so far exhibited small spin injection efficiencies at room temperature (RT).[23–26] This ineffectiveness most likely results from the impedance mismatch between the (high-resistance) SC and the (low-resistance) FM in the diffusive regime.[27–29]

One way to circumvent the impedance mismatch problem is to use a tunnel barrier at the SC/FM interface.[28,29] The intrinsic Schottky barrier formed at the SC/FM interface[23,25,26] or additional insulating tunnel barriers[24] represent promising options in this context, but high spin injection efficiencies are restricted to low temperatures. This raises the question whether alternative ferromagnetic conductors can be found with resistances larger than that typical for FM's with identical or higher spin polarizations. $Fe_3Si$ is one such candidate: although the calculated density of states[30–33] for bulk $Fe_3Si$ does not predict half-metallic behavior, the DOS close to the Fermi level exhibits a dip for the minority spins and the spin polarization should be roughly of the same order of magnitude[32] as that for Fe, $\approx 43\%$.[21] A striking advantage of $Fe_3Si$ is that the growth is easier to control, as compared to the ternary Heusler alloys, due to its binary nature and due to the fact that the phase diagram of the ordered alloy ($\alpha'$) is relatively broad with Si contents ranging from 9.5 to 26 at. % Si.[34,35] Crystallographically similar to the Heusler alloys, $Fe_3Si$ is a ferromagnet with a Curie temperature $T_C=803$ K and a lattice parameter of 5.642 Å, which can be stabilized in the cubic $L2_1$ structure.[34–36] The cubic $L2_1$ structure with the composition $X_2YZ$ has four penetrating fcc sublattices. The $X$ atoms occupy two sublattices with the origins at $(1/4,1/4,1/4)$ and $(3/4,3/4,3/4)$ and the $Y$ and $Z$ atoms are positioned at $(0,0,0)$ and $(1/2,1/2,1/2)$ sublattices, respectively. $Fe_3Si$ has two nonequivalent Fe sites with magnetic moments $\mu_{Fe^I}=2.2\mu_B$ per atom and $\mu_{Fe^{II}}=1.35\mu_B$ per atom and is therefore sometimes referred to as $Fe_2^{II}Fe^ISi$. Moreover, the Si site has a magnetic moment of $\mu_{Si}=-0.07\mu_B$ per atom.[37] Since $Fe_3Si$ is nearly lattice matched to GaAs(−0.21%), it can be grown epitaxially on GaAs(001). Only a few studies on the growth and magnetic properties of thin films have been reported thus far.[38–44] A further advantage of $Fe_3Si$/GaAs(001) heterostructures relates to their thermal stability upon postgrowth annealing as reported by Hsieh *et al.*[39] and Noh *et al.*,[41] as compared to Fe/GaAs(001).[45,46] Here we report experimental results on the structural, magnetic, electronic, and spin transport properties of $Fe_3Si$/GaAs(001), which indicate the possibility of using these heterostructures in future device applications.

## II. RESULTS

The growth and the *in situ* measurements were carried out in an ultrahigh vacuum molecular beam epitaxy (MBE) chamber combining a low-energy electron diffraction (LEED) and magneto-optic Kerr effect (MOKE) setup, with a base pressure of $3\times10^{-10}$ mbar. The substrate consists of a commercial Si *n*-doped GaAs(001) wafer ($n=10^{24}$ m$^{-3}$), where a buffer layer ($\approx0.5$ $\mu$m) of homoepitaxial GaAs was grown in another (semiconductor) MBE chamber (in order to provide a smooth surface) and capped with As. After transferring the GaAs substrate to the metal MBE chamber the As cap was removed by annealing at $T\approx430$ °C for 15 min. Subsequently the temperature was increased to $T\approx570$ °C for 30 min in order to obtain a clean and ordered surface before the $Fe_3Si$ growth. This treatment leads to a "pseudo" $(4\times6)$ reconstructed GaAs(001) surface. The stoichiometric $Fe_3Si$ film was obtained by coevaporation of Fe and Si at a constant temperature $T\approx300$ °C with a growth rate of 0.36 nm/min. The deposition was monitored with a quartz microbalance. To prevent oxidation of the film for *ex situ* measurements the sample was capped with a 1.8 nm thick Au layer.[43] The surface reconstruction of the substrate and the deposited film was examined with a VG rearview LEED system. Figure 1(a) shows a LEED image of "pseudo" ($P4\times6$) reconstructed GaAs(001) surface. While the $6\times$ reconstruction spots are clear and visible, the $4\times$ reconstruction spots are missing. However, $2\times$ and $3\times$ intermediate streaks along the $[1\bar{1}0]$ are apparent. This surface reconstruction is a

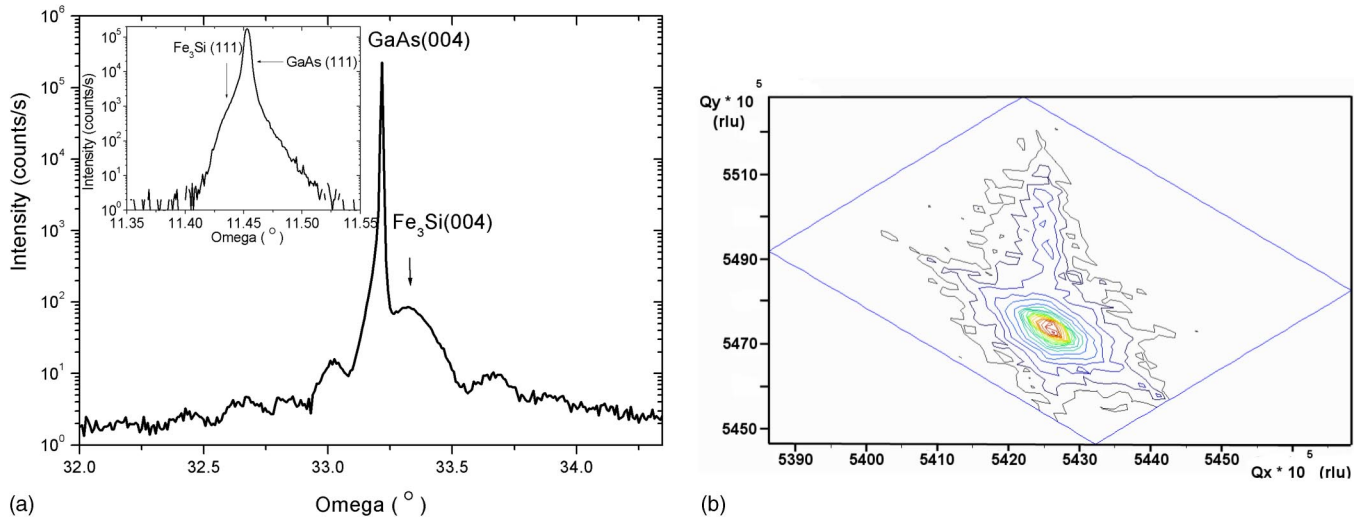


FIG. 2. (a) X-ray (004) diffraction peak $\omega/2\theta$ scan of the 21 nm thick $Fe_3Si/GaAs(001)$ sample. The inset shows an $\omega/2\theta$ scan around the (111) peak of the same sample. (b) The reciprocal space map at the (404) diffraction peak, given in reciprocal lattice units, indicates that the $Fe_3Si$ film is, at this thickness, still fully strained in plane.

transient phase between the As-rich $(2\times4)$ and the Ga-rich $(4\times2)$ phases.[47] Furthermore, the image indicates that the surface was clean and well ordered prior to the growth of the $Fe_3Si$ film. Figure 1(b) is the LEED image of a 74 monolayer (ML) (21 nm) thick $Fe_3Si$ film. The diffraction spots exhibit the expected $(1\times1)$ reconstructed surface of the cubic $L2_1$ structure.

Further structural characterization was performed *ex situ* by high-resolution x-ray diffraction. The (004) and (111) $\omega/2\theta$ scans and (404) reciprocal space map (RSM) were collected in continuous mode on a PANalytical PW3050/65 high-resolution diffractometer using Cu $K\alpha$ radiation with a parabolic graded mirror, a four-bounce Ge(220) monochromator, a triple-bounce analyzer crystal, and a dwell time of 20 s. The PANalytical software EPITAXY 4 was used to analyze the experimental data. An x-ray $\omega/2\theta$ scan around the GaAs(004) diffraction peak is presented in Fig. 2(a). At $\omega=33.2°$ we find the sharp diffraction peak from the GaAs(004) plane while the $Fe_3Si(004)$ layer peak is visible at $\omega\approx33.3°$. The $Fe_3Si$ layer peak is relatively broad and weak as compared to the GaAs peak and its position cannot be determined very accurately. However, a full width at half maximum of $\approx0.17°$ implies a crystallite size similar to the film thickness [21 nm from x-ray reflectometry (XRR)[43]] and thus very few crystalline defects or grain boundaries. Furthermore, the presence of distinct interference fringes up to the fourth order indicates that the interface between substrate and the $Fe_3Si$ film is reasonably sharp. Figure 2(b) presents a RSM taken at the (404) diffraction peak. The diagonal streak is a feature of the analyzer, caused by finite angular resolution.[48] The reciprocal space map yields information about the film stress. As can be seen from the vertical streak, the 21 nm $Fe_3Si$ film is still fully strained in-plane at this thickness, which means that the in-plane lattice parameters of the film are matched to the substrate lattice parameter. The (004) scan yields an "experimental x-ray mismatch" (out-of-plane lattice mismatch) of $\eta^*=-0.0029$. This is related, to first order of approximation, to the true lattice mismatch by[48]

$$\eta=\eta^*\times\frac{1-\nu}{1+\nu}, \tag{1}$$

where $\nu\approx0.395$ is the Poisson ratio determined by using the stiffness constants published by Kötter *et al.*[49] The equilibrium lattice mismatch can thus be determined from the lattice mismatch definition,

$$\eta=\frac{a_l-a_s}{a_s}, \tag{2}$$

where $a_l$ and $a_s$ are the equilibrium lattice constants of the $Fe_3Si$ and the substrate (GaAs), respectively. We calculate for the 21 nm $Fe_3Si$ sample the stoichiometric composition as $24.4\pm0.2$ at. % Si by applying Vegard's law[50] to the bulk lattice parameter results available in the literature.[34,51] This result indicates an almost stoichiometric sample (25 at. % Si).[52] The inset of Fig. 2(a) presents a $\omega/2\theta$ scan around the (111) diffraction peak, which was measured by means of a 55° offset in $\psi$ (tilt angle). The shoulder inside the GaAs(111) peak represents the $Fe_3Si(111)$ diffraction peak. The latter only appears if the ordered space group $Fm\bar{3}m$ has been stabilized. In the case of Si randomly diluted in bcc Fe in the space group $Im\bar{3}m$, the $Fe_3Si(111)$ diffraction peak does not exist, as for low Si concentrations (<9.5 at. %) or the case of the closely related meteoritical mineral suessite.[53]

Polarized neutron reflectometry (PNR) experiments were carried out on the neutron reflectometer CRISP at the Rutherford Appleton Laboratory. Measurements were taken at RT with a 4.5 kOe magnetic field applied in plane ([110] ) along the direction normal to the scattering plane using an electromagnet. Previous superconducting quantum interference device (SQUID) measurements confirm that this field is sufficient to saturate the film in the plane (see Fig. 4 below). The neutrons were polarized by reflection from an Fe-Co -V:$TiN_x$ supermirror and were collimated by two sets of slits; the polarized beam was then reflected by the sample and the spin up and down reflected intensities measured us-

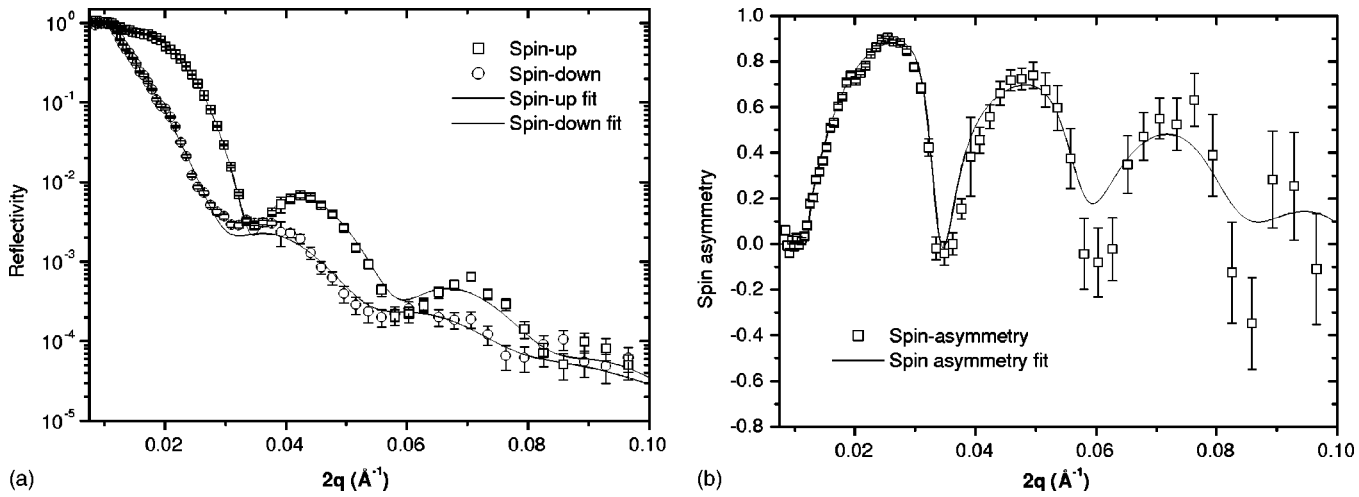


FIG. 3. (a) PNR spectra of the 21 nm $Fe_3Si/GaAs(001)$ sample. The boxes and circles are the experimental data, while the straight lines indicate the fit for the spin up and down reflectivities. (b) The spin asymmetry is the normalized difference between spin up and down reflection and the corresponding fit is an indication of the quality of the reflectivity fits to the measured data. The line represents the fit to the data.

ing a single $^3$He detector. The longitudinal momentum transfer $2q$ (determined by a time-of-flight method) varied from $\approx 0.006$ to $\approx 0.1$ Å$^{-1}$ and was collected using three incident angles from 0.45° to 1.2°. The polarization of the incident beam (97%) was reversed by means of a Drabkin two-coil nonadiabatic spin flipper every 5 min throughout the measurements (see Ref. 54 for further details of the experimental setup). The raw spectra obtained were corrected for the polarizer, flipper, and detector efficiencies and fitted using a slab layer model.[55,56] Parameters of the fit include the magnetic moment per atom, roughness, mass densities, layer thickness, nuclear scattering length, wavelength resolution, the number of layers, and a scaling factor that corrects the spectrum for misalignments of the sample. In order to reduce the number of fitting parameters, bulk values were assumed for the nuclear scattering lengths and we confirmed thickness and roughness values by means of XRR, published previously.[43] Figure 3(a) shows the normalized polarized neutron reflectivity data of the 21 nm $Fe_3Si/GaAs(001)$ sample for spin up and down neutron states. The solid lines represent the fits to the data. The amplitude of the reflectivity fringes is determined by the nuclear contrast between the different layers (arising from the nuclear as well as magnetic potential) while the period is determined by the different layer thicknesses and the drop in overall intensity is affected by the presence of interface roughness. PNR allows us, therefore, to determine simultaneously the moments, thicknesses, and interface roughnesses. The best fit yields a thickness of $21.63 \pm 0.05$ nm, an $Fe_3Si/GaAs$ interface roughness of $2.3 \pm 0.1$ nm, and a magnetic moment of $(1.107 \pm 0.014)\mu_B$ per atom at RT, which is very close to the bulk value of $1.175\mu_B$ per atom at 6.5 K.[37,57–59] Furthermore, the fit indicates a Au capping layer thickness of $2.0 \pm 0.1$ nm. Figure 3(b) presents the spin asymmetry, which is the normalized difference between spin up and down reflectivities. The spin asymmetry gives an indication of the quality of the reflectivity fits and it shows that the fit follows closely the data even up to higher momentum transfer values.

In addition to the PNR measurements, SQUID magnetometry measurements (Quantum Design MPMS) were performed in order to determine the magnetic moment per atom at different temperatures. Figure 4 shows the SQUID data with the magnetic field applied along the $[1\bar{1}0]$ direction for the 21 nm thick film. The magnetic moments thus obtained are $(0.9 \pm 0.1)\mu_B$ per atom at RT and $(1.0 \pm 0.1)\mu_B$ per atom at 10 K for the $Fe_3Si$ film. Furthermore, the coercive field for this direction is $\approx 7.5$ Oe and the film is saturated in plane along the hard axis direction already at 200 Oe.

To estimate the anisotropy constants $K_1$ and $K_U$ we have performed longitudinal vector MOKE measurements *ex situ*.[60] A polar plot of the magnetizing energy $\omega_m$ as determined by the integration of the magnetization curves is given in Fig. 5(a). The polar plot of $\omega_m$ shows a dominant fourfold (cubic) component. The in-plane fourfold magnetic easy axes are along the in-plane $\langle 100 \rangle$ directions relative to the GaAs(001) surface. A fit of $\omega_m(\phi)$ to the expression

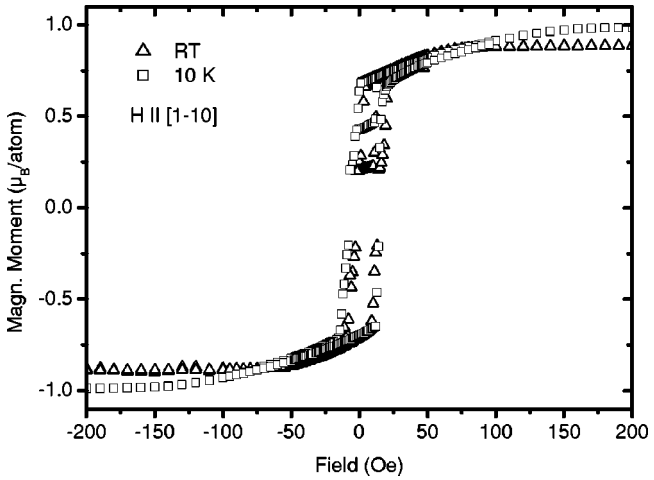


FIG. 4. Two hard axis hysteresis loops of the 21 nm sample measured at RT (triangles) and 10 K (boxes) with the magnetic field applied along the $[1\bar{1}0]$ direction.

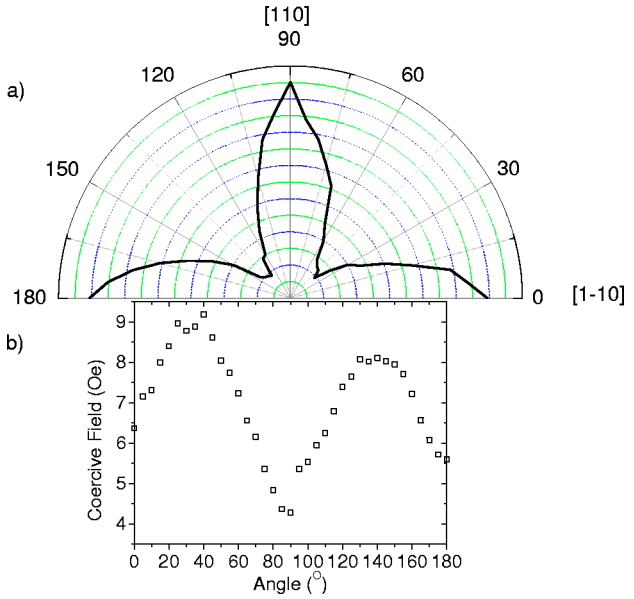


FIG. 5. (a) Polar plot of the magnetizing energy $\omega_m$ for the 21 nm $Fe_3Si/GaAs(001)$ sample obtained from longitudinal vector MOKE measurements (due to the symmetry of the plot, only half of the polar plot is shown). (b) Coercive field versus angle of the magnetic field showing that the two hard and easy axes are slightly nonequivalent (the 0° is relative to the $[1\bar{1}0]$ direction).

$$\omega_m(\phi) = -\frac{K_1}{4}\sin^2(2\phi) + K_U \sin^2(\phi), \tag{3}$$

where $\phi$ is measured from the $[1\bar{1}0]$ direction in analogy to measurements on Fe/GaAs(001) structures,[61] yields the effective anisotropy constants $K_1 = (3.1 \pm 0.6) \times 10^4$ erg/cm$^3$ and $K_U = -(4.6 \pm 0.9) \times 10^2$ erg/cm$^3$. $K_1$ is in good agreement with the bulk value, $K_1^{\text{bulk}} = 5.4 \times 10^4$ erg/cm$^3$.[62] The negative sign for $K_U$ indicates that the uniaxial easy axis is along the [110] direction, as in the Fe/GaAs(001) heterostructure system.[61] However, $K_U$ is two orders of magnitude smaller than the cubic anisotropy constant and has little influence on the magnetizing energy $\omega_m(\phi)$ for this $Fe_3Si$ film thickness. Herfort *et al.*[42] mention a slight non-equivalence between the orientations $[1\bar{1}0]$ and [110] of the two hard axes, which is also apparent in our sample due to a higher magnetizing energy along the [110] direction. We also observe this nonequivalence in coercivity along the hard and easy axis directions as shown in Fig. 5(b).

The spin-dependent transport measurements were carried out using optical spin orientation where electrons are photoexcited in the GaAs substrate with spin polarization dependent on the incident light helicity.[63] For this purpose, an Ohmic NiGeAu bottom contact was added to the structure (see Ref. 64 for details about the preparation and growth of the bottom contact) and two electrical top contacts were grown by thermal evaporation of 200 nm thick Al pads on the Au capping layer (all reported measurements were carried out at RT). The two top contacts and the back contact were used for conventional three-point-geometry *I-V* measurements which showed a Schottky diode behavior with a barrier height of 0.51 eV.[43] For the photoexcitation measurements an in-plane setup was used with the magnetic field applied along the easy axis and the light incident at an angle $\theta$=45° from the sample surface normal. At this angle of incidence the photon helicity, and therefore the spin polarization of the excited electrons, have an in-plane component parallel to the FM layer magnetization. For a range of applied bias, the spin polarized electrons which tunnel into the FM are filtered at the SC/FM interface according to their polarization with respect to the FM layer magnetization.[65] In our setup we use a photoelastic modulator (operated at 50 kHz) to alternate from right- to left-circularly polarized light and a lock-in technique to measure the corresponding modulation in the current $\Delta I$. This helicity-dependent photocurrent has a magneto-optic contribution $I_{\text{MCD}}$ due to magnetic circular dichroism (MCD), besides the spin filtering contribution $I_{\text{SF}}$. The fact that $I_{\text{MCD}}$ is proportional to the photocurrent $I_{\text{ph}}$ as measured with linearly polarized light is used in order to account for the MCD contribution.[65] If $\alpha$ is the constant of proportionality, $I_{\text{MCD}} = \alpha I_{\text{ph}}$, then

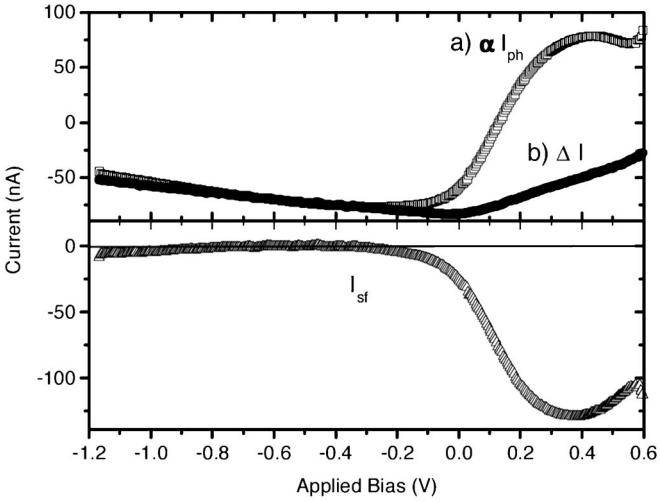


FIG. 6. Measurements of the scaled photocurrent $\alpha I_{\text{ph}}$ (a), helicity-dependent photocurrent $\Delta I$ (b), and pure spin filtering contribution $I_{\text{SF}}$ (bottom) with $\alpha = 51.5 \times 10^{-3}$ (see text). $I_{\text{SF}}$ is negligible at reverse bias and becomes finite for forward bias, which we attribute to spin-dependent tunneling of electrons from the SC into the FM.

$$\Delta I = I_{\text{MCD}} + I_{\text{SF}} \Rightarrow I_{\text{SF}} = \Delta I - \alpha I_{\text{ph}}. \tag{4}$$

For the *n*-type Schottky barrier structure used, we expect all the photoexcited electrons to travel toward the SC back contact at sufficient reverse bias, in which case $\Delta I$ is only due to MCD since no photoexcited electrons pass through the FM layer. Therefore, $\alpha$ is determined by the ratio of $I_{\text{ph}}$ and $\Delta I$ for this reverse bias range up to the breakdown of the diode. Figure 6 shows the measurements for $\alpha I_{\text{ph}}$, $\Delta I$, and $I_{\text{SF}}$ with $\alpha = 51.5 \times 10^{-3}$. As expected, $|I_{\text{SF}}|$ is zero for reverse bias whereas for forward bias where the probability for tunneling into the FM layer is progressively increased, $|I_{\text{SF}}|$ is nonzero and peaks at 0.38 V. Surprisingly, $I_{\text{ph}}$ exhibits a dip at 0.57 V, which has only been previously reported for tunnel-

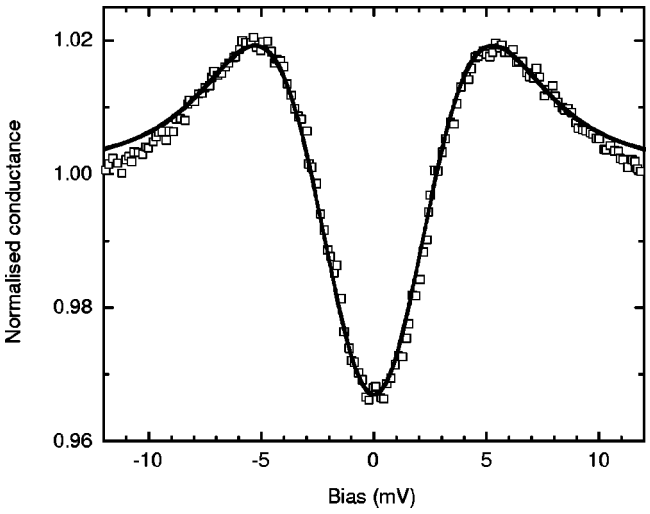


FIG. 7. The normalized conductance versus applied bias as measured with Andreev reflection. The fit (straight line) to a generalized BTK model gives a spin polarization of $P=(45\pm5)\%$.

ing barrier structures,[65] but not for a SC/FM Schottky barrier interface.[64]

In addition to the spin-dependent measurements the Van der Pauw[66] method was used to measure the resistivity of the $Fe_3Si$ sample with four copper probes lowered onto the Au capping layer. Electric current flowing through the semiconductor is negligible (this was checked by repeating the measurements with a negative bias between the top and bottom electrodes, showing no significant alterations to the measured resistivity). The sample was treated as two sheet resistors in parallel (Au and $Fe_3Si$) in order to extract the value for $Fe_3Si$ from the effective overall value of the multilayer. A value of $(4.1\pm0.7)\times10^{-7}$ $\Omega$ m is obtained which compares well with the resistivity of $3.8\times10^{-7}$ $\Omega$ m for bulk $Fe_3Si$.[67] For comparison, the resistivity of our *n*-type doped GaAs substrate is about $2\times10^{-5}$ $\Omega$ m.[68]

Point contact Andreev reflection spectroscopy was performed in order to measure the spin polarization of the transport current of the $Fe_3Si$ film. Ten spectra have been obtained at 4.2 K, with the superconducting Nb tip contacting the sample at different locations. The normalized conductance spectra were analyzed using the generalization of the Blonder-Tinkham-Klapwijk (BTK) model for spin polarized materials.[69] The spectra are relatively broad due to interface scattering in the junction between the tip and the sample. As has been shown elsewhere,[70] in this regime only the upper bound for the spin polarization can be inferred from the fitting. The upper bound varies between $P=25\%$ and 55% at different locations on the sample surface. This is quite likely due to a variation in interface properties because of the gold cap. For one data set (which had the smallest broadening), the fitting procedure yielded $P=(45\pm5)\%$ (Fig. 7). The other parameters from the fitting yield a value for the superconducting gap $\Delta_{Nb}=1.50\pm0.05$ meV, a dimensionless interface parameter $Z=0.50\pm0.05$, and a smearing parameter $\omega=2.54$ meV. The normal state (when Nb is a normal conductor) resistance was measured as $R_0=37.7$ $\Omega$.

## III. DISCUSSION

For the growth we have chosen the Ga-rich $(P4\times6)$ reconstructed GaAs(001) surface, which can be stabilized by annealing the GaAs substrate to $\approx$823 K prior to the growth,[71] to avoid As segregation into the $Fe_3Si$ film. However, segregation of As and Ga into the $Fe_3Si$ film seems unlikely as has been shown by means of synchrotron x-ray studies.[41] Indeed, Herfort *et al.*[42,44] report high-quality epitaxial films stabilized even on the As-rich GaAs(001)-$2\times1$ surface. The LEED pattern of the 74 ML film exhibits the $(1\times1)$ reconstructed surface of the $L2_1$ structure. We have reported before[43] the appearance of this LEED pattern at 3.7 ML. In addition, Refs. 40, 42, and 44 describe the appearance of reflection high-energy electron diffraction patterns already at 1 ML and sharp Kikuchi arcs at $\approx$12 ML, thereby indicating a two-dimensional (2D) growth mode. After the deposition of 74 ML we cannot detect any $c(1\times1)$ or $c(2\times2)$ surface reconstruction due to Si enrichment of the surface as reported previously[72–74] for bulk $Fe_3Si$ after annealing at temperatures of $673\leqslant T\leqslant953$ K. The two Si-rich phases are reported to be temperature reversible unless quenched (e.g., for bulk[72] down from 823 to 473 K at 350 K/min). The growth of the back contact for the spin transport measurement (photoexcitation) studies required a postgrowth anneal to 703 K followed by a cooling process at 50 K/min to 473 K in a rapid thermal annealer and therefore we cannot exclude the possibility of a Si enrichment in the top 2–3 ML of the $Fe_3Si$ film. The appearance of Pendellösung fringes and the relatively sharp $Fe_3Si$ peak in our (004) x-ray diffraction $\omega/2\theta$ scan indicate that high-quality epitaxial films have been grown with smooth interfaces in good agreement with our x-ray reflectometry data.[43] The (111)GaAs diffraction peak as seen in our (111) $\omega/2\theta$ scan surprisingly exhibits a shoulder peak toward a smaller angle and not as would be expected from the (004) scan toward a higher angle. Epitaxial relations for $Fe_3Si[1\bar{1}0]\|GaAs[1\bar{1}0]$ and $Fe_3Si(001)\|GaAs(001)$ have been reported by Hong *et al.*[38] and Hsieh *et al.*[39] Furthermore, our LEED pictures present a clear proof that the desired $(\alpha')$ phase crystallized in the cubic $L2_1$ structure has been stabilized. Therefore, we attribute this shoulder in the GaAs(111) peak to local changes in the stoichiometry of the $Fe_3Si$ film or to the single-crystalline quality of the GaAs substrate. If the latter were the case, then the $Fe_3Si(111)$ peak would not be visible due to the reduced intensity of this diffraction peak as compared to the GaAs(111) peak. The RSM shows that the film is fully strained in-plane and relaxed in the out-of-plane direction leading to a tetragonal distortion as reported also by other groups.[39,41,42] Strain relaxation of the $Fe_3Si/GaAs$ interface has so far only been reported for growth temperatures exceeding 773 K or after extensive postannealing ($\approx$24 h).[39] Regarding the interface roughnesses and layer thicknesses, the results of the PNR fits are in relatively good agreement with our XRR results.[43] However, we obtain different values for the $Fe_3Si/GaAs$ interface roughness from the PNR and XRR fits. Since the XRR measurement extends to higher-momentum-transfer values and hence exhibit more fringes we are more confident about the value given by XRR,

$0.7 \pm 0.1$ nm.[43] In addition, the GaAs buffer layer deposited prior to the $Fe_3Si$ growth should provide a relatively smooth surface as has been shown by the LEED results. Electron microscopy studies are being conducted at the moment to clarify this roughness discrepancy. Furthermore, different changes in density from the bulk value[75] (7.192 $gcm^{-3}$) are suggested by XRR (+5%) and PNR (−20%). However, the tetragonal distortion of the film can only account for a change of −1.5%. This may be related to atomic disorder in the film, which changes the respective scattering factors. The scattering factors (x-ray and nuclear) are closely related to the density of the materials in the fits for XRR and PNR measurements. A slight Fe and Si site disorder has already been suggested by Paoletti and Passari[57] for stoichiometric bulk $Fe_3Si$ and shown to exist by means of neutron diffraction by Pickart *et al.*[76] An indication of some site disorder is given also by the value of the resistivity, which is slightly higher than for bulk. Another explanation is that our film is slightly off stoichiometry; as Herfort *et al.*[42] have pointed out, there is a large discrepancy in the literature about the "real" lattice constant of the stoichiometric $Fe_3Si$ intermetallic compound. Regarding the total magnetic moment of the film the value yielded by the PNR measurements is closer to the bulk value[37,57–59] or values given for films[40,42] than the value obtained from SQUID magnetometry. The sensitivity of PNR to the magnetic moment of the single atom rather than to the volume magnetization, which is the case for SQUID magnetometry, makes it a more reliable source to determine this observable. Vector MOKE measurements indicate the presence of an in-plane uniaxial contribution in addition to the dominant in-plane cubic anisotropy. The coercivity of our sample (21 nm thick) is higher than the value reported in Ref. 42 for their 33 nm thick sample. Coercive fields are typically smaller in thicker films so that a difference in thickness could yield a different value; also our growth temperature was slightly higher[43] than the optimal growth temperature suggested by Herfort *et al.*,[42] which could result in more defects in our film leading to more pinning sites and therefore to a larger coercive field. However, comparison with the results of Liou *et al.*[40] shows that our film exhibits a coercivity along the [110] direction four times smaller than their extrapolated value for a 21 nm sample. For Schottky barrier interfaces spin filtering is expected to occur due to the tunneling process of electrons through the barrier.[65] This agrees well with the measured $|I_{SF}|$, which shows a peak where tunneling is most probable. Thus we attribute the obtained $I_{SF}$ to spin-dependent tunneling across the Schottky barrier at the SC/FM interface. This result demonstrates spin detection by the ferromagnetic $Fe_3Si$. Furthermore, the measurements indicate an anomalous feature for a single film on GaAs. As mentioned before, a dip (at 0.57 V) in $\alpha I_{ph}$ has only been previously reported for artificial tunneling barrier structures. A possible explanation could be the enrichment of the top monolayers of the $Fe_3Si$ film with Si (as reported previously for bulk[72–74] ) at the GaAs interface, due to the annealing and cooling treatment for the back contact, leading to an artificial tunnel barrier at the interface. This segregation of Si toward the surface is at first sight an undesired phenomenon, but it could be used to circumvent the conductivity mismatch between SC/FM by creating a higher-resistance region at the interface than in the film. This topic is under further investigation and the results will be published elsewhere. The value of the resistivity of $Fe_3Si$ is another interesting point in the context of the conductivity mismatch. Even though we show that our film exhibits bulk behavior, it must be mentioned that the resistivity of the stoichiometric $Fe_3Si$ is roughly only four times higher than that of pure Fe,[67] which would not necessarily lead to a huge increase in spin injection efficiency. However, site disorder in the $L2_1$ structure for Fe-rich $\alpha'$ compounds with $\approx$20 at. % Si leads to an increase by a factor of $\approx$10 in the electrical resistivity[36] at RT to $\approx$75 (Ref. 67) in residual electrical resistivity (0 K) as compared to pure Fe. Si surface segregation after special postgrowth treatment together with an increased resistivity for off-stoichiometric samples make this a very promising compound for future spintronic devices. The Andreev reflection measurements yield a polarization of the transport current $P=(45\pm5)\%$. This is of the same order of magnitude as measurements on Fe as is anticipated from DOS calculations.[30–33] The Andreev reflection measurements reinforce the point that $Fe_3Si$ is likely to be a good candidate for spin injection into GaAs even though it exhibits no half-metallic behavior.

## IV. CONCLUSIONS

We have studied the structural, magnetic, electronic, and spin transport properties of a 21 nm thick $Fe_3Si$ film grown on GaAs(001). LEED pictures show an ordered $(1\times1)$ $Fe_3Si(001)$ surface, while high-resolution x-ray diffraction data indicate an almost stoichiometric film. The film is lattice matched in-plane to the GaAs substrate and therefore slightly tetragonal distorted as evidenced by the (404) RSM. Furthermore, the film has a bulklike moment as measured by PNR and exhibits magnetic cubic anisotropy with the in-plane easy axes along the $\langle100\rangle$ directions. Photoexcitation studies based on optical spin orientation demonstrate spin detection in this FM alloy at RT in the tunneling regime, e.g., for sufficient positive applied bias values. The resistivity value is close to the $Fe_3Si$ bulk value. In addition, Andreev reflection yields a transport spin polarization of $P=(45\pm5)\%$. These results suggest that $Fe_3Si/GaAs(001)$ heterostructures are promising candidates for future spintronics applications.

## ACKNOWLEDGMENTS

We thank H. E. Beere and D. A. Ritchie for the growth of the GaAs buffer layer and S. J. Steinmüller for helpful discussions. Furthermore, we acknowledge financial support from the EPSRC (U.K.). T.T. expresses his gratitude to the Cambridge Commonwealth Trust for funding. H.G.-M. is grateful to the Secretaria de Estado de Educación y Universidades (Spain) for financial support. A. I. wishes to express his gratitude to the Cambridge European Trust and Nordiko Ltd. for financial support.

*Present address: Department of Electronic Engineering Sensor and Magnetism Group, Polytechnic University of Valencia, Valencia, 46022, Spain.
†Corresponding author. FAX: +44(0)1223350266. Email address: jacb1@phy.cam.ac.uk

[1] F. Heusler, Verh. Dtsch. Phys. Ges. **5**, 219 (1903).
[2] J. S. Moodera, L. R. Kinder, T. M. Wong, and R. Meservey, Phys. Rev. Lett. **74**, 3273 (1995).
[3] S. Kämmerer, S. Heitmann, D. Meyners, D. Sudfeld, A. Thomes, A. Hütten, and G. Reiss, J. Appl. Phys. **93**, 7945 (2003).
[4] M. C. Kautzky, F. B. Mancoff, J. F. Bobo, P. R. Johnson, R. L. White, and B. M. Clemens, J. Appl. Phys. **81**, 4026 (1997).
[5] R. A. de Groot, F. M. Mueller, P. G. van Engen, and K. H. J. Buschow, Phys. Rev. Lett. **50**, 2024 (1983).
[6] V. Y. Irkhin and M. I. Katsnel'son, Phys. Usp. **37**, 659 (1994).
[7] J. Kübler, A. R. Williams, and C. B. Sommers, Phys. Rev. B **28**, 1745 (1983).
[8] S. Fujii, S. Sugimura, S. Ishida, and S. Asano, J. Phys.: Condens. Matter **2**, 8583 (1990).
[9] S. Ishida, T. Masaki, S. Fujii, and S. Asano, Physica B **239**, 163 (1997).
[10] S. Fujii, S. Ishida, and S. Asano, J. Phys. Soc. Jpn. **63**, 1881 (1994).
[11] M. P. Raphael, B. Ravel, M. A. Willard, S. F. Cheng, B. N. Das, R. M. Stoud, K. M. Bussmann, J. H. Claassen, and V. G. Harris, Appl. Phys. Lett. **79**, 4396 (2001).
[12] U. Geiersbach, A. Bergmann, and K. Westerholt, J. Magn. Magn. Mater. **240**, 546 (2002).
[13] U. Geiersbach, A. Bergmann, and K. Westerholt, Thin Solid Films **425**, 225 (2003).
[14] L. J. Singh, Z. H. Barber, Y. Miyoshi, Y. Bugoslavsky, W. R. Branford, and L. F. Cohen, Appl. Phys. Lett. **84**, 2367 (2004).
[15] L. J. Singh, Z. H. Barber, Y. Miyoshi, W. R. Branford, and L. F. Cohen, J. Appl. Phys. **95**, 7231 (2004).
[16] P. J. Brown, K. U. Neumann, P. J. Webster, and K. R. A. Ziebeck, J. Phys.: Condens. Matter **12**, 1827 (2000).
[17] S. Ishida, S. Fujii, S. Kashiwagi, and S. Asano, J. Phys. Soc. Jpn. **64**, 2152 (1995).
[18] S. Ishida, T. Masaki, S. Fujii, and S. Asano, Physica B **245**, 1 (1998).
[19] P. J. Webster, J. Phys. Chem. Solids **32**, 1221 (1971).
[20] D. Orgassa, H. Fujiwara, T. C. Schulthess, and W. H. Butler, Phys. Rev. B **60**, 13 237 (1999).
[21] R. J. Soulen, Jr., J. M. Byers, M. S. Osofsky, B. Nadgorny, T. Ambrose, S. F. Cheng, P. R. Broussard, C. T. Tanaka, J. Nowak, J. S. Moodera, A. Barry, and J. M. D. Coey, Science **282**, 85 (1998).
[22] P. A. Dowben and R. Skomski, J. Appl. Phys. **95**, 7453 (2004).
[23] H. J. Zhu, M. Ramsteiner, H. Kostial, M. Wassermeier, H. P. Schönherr, and K. H. Ploog, Phys. Rev. Lett. **87**, 016601 (2001).
[24] V. F. Motsnyi, J. D. Boeck, J. Das, W. V. Roy, G. Borghs, E. Goovaerts, and V. I. Safarov, Appl. Phys. Lett. **81**, 265 (2002).
[25] A. T. Hanbicki, B. T. Jonker, G. Itskos, G. Kioseoglou, and A. Petrou, Appl. Phys. Lett. **80**, 1240 (2002).
[26] A. T. Hanbicki, O. M. J. van't Erve, R. Magno, G. Kioseoglou, C. H. Li, B. T. Jonker, G. Itskos, R. Mallory, M. Yasar, and A. Petrou, Appl. Phys. Lett. **82**, 4092 (2003).
[27] G. Schmidt, D. Ferrand, L. W. Molenkamp, A. T. Filip, and B. J. van Wees, Phys. Rev. B **62**, R4790 (2000).
[28] G. Schmidt and L. W. Molenkamp, Semicond. Sci. Technol. **17**, 310 (2002).
[29] E. I. Rashba, Phys. Rev. B **62**, R16 267 (2000).
[30] J. Kudrnovsky, N. E. Christensen, and O. K. Andersen, Phys. Rev. B **43**, 5924 (1991).
[31] S. Fujii, S. Ishida, and S. Asano, J. Phys. Soc. Jpn. **64**, 185 (1995).
[32] E. G. Moroni, W. Wolf, J. Hafner, and R. Podloucky, Phys. Rev. B **59**, 12 860 (1999).
[33] A. Bansil, S. Kaprzyk, P. E. Mijnarends, and J. Tobola, Phys. Rev. B **60**, 13 396 (1999).
[34] A. Ôsawa and T. Murata, Nippon Kinzoku Gakkaishi **4**, 228 (1940).
[35] M. Hansen, *Fe-Si Iron-Silicon* (McGraw-Hill, New York, 1958), Vol. I.
[36] R. M. Bozorth, *Ferromagnetism* (D. Van Nostrand Company, New York, 1951).
[37] W. A. Hines, A. H. Menotti, J. I. Budnick, T. J. Burch, T. Litrenta, V. Niculescu, and K. Raj, Phys. Rev. B **13**, 4060 (1976).
[38] M. Hong, H. S. Chen, J. Kwo, A. R. Kortan, J. P. Mannaerts, B. E. Weir, and L. C. Feldman, J. Cryst. Growth **111**, 984 (1991).
[39] Y. F. Hsieh, M. Hong, J. Kwo, A. R. Kortan, H. S. Chen, and J. P. Mannaerts, in *GaAs and Related Compounds 1991*, edited by G. B. Stringfellow, IOP Conf. Ser. No. 120 (Institute of Physics, London, 1992), p. 95.
[40] S. H. Liou, S. S. Malhorta, J. X. Shen, M. Hong, J. Kwo, H. S. Chen, and J. P. Mannaerts, J. Appl. Phys. **73**, 6766 (1993).
[41] D. Y. Noh, Y. Hwu, J. H. He, M. Hong, and J. P. Mannáerts, Appl. Phys. Lett. **68**, 1528 (1996).
[42] J. Herfort, H. P. Schönherr, and K. H. Ploog, Appl. Phys. Lett. **83**, 3912 (2003).
[43] A. Ionescu, C. A. F. Vaz, T. Tripiniotis, C. M. Gürtler, M. E. Vickers, H. García-Miquel, and J. A. C. Bland, J. Magn. Magn. Mater. **286**, 72 (2005).
[44] J. Herfort, H. P. Schönherr, K. J. Friedland, and K. H. Ploog, J. Vac. Sci. Technol. B **22**, 2073 (2004).
[45] E. M. Kneedler, B. T. Jonker, P. M. Thibado, R. J. Wagner, B. V. Shanabrook, and L. J. Whitman, Phys. Rev. B **56**, 8163 (1997).
[46] G. Wedler, B. Wassermann, R. Nötzel, and R. Koch, Appl. Phys. Lett. **78**, 1270 (2001).
[47] Q. K. Xue, T. Hashizume, and T. Sakurai, Appl. Surf. Sci. **141**, 244 (1999).
[48] B. K. Bowen and B. K. Tanner, *High Resolution X-ray Diffractometry and Topography* (Taylor & Francis, London, 1998).
[49] G. Kötter, K. Nembach, F. Wallow, and E. Nembach, Mater. Sci. Eng., A **114**, 29 (1989).
[50] L. Vegard, Z. Phys. **5**, 17 (1921).
[51] M. C. M. Farquhar, H. Lipson, and A. R. Weill, J. Iron Steel Inst., London **152**, 457 (1945).
[52] Throughout the text our results for thin films are compared with values for bulk samples, even though we expect a larger degree of disorder in our system due to film strain and constraints in the annealing procedure as compared to bulk samples.
[53] K. Keil, J. L. Berkly, and L. H. Fuchs, Am. Mineral. **67**, 126 (1982).
[54] J. Penfold, Physica B **173**, 1 (1991).
[55] S. J. Blundell and J. A. C. Bland, Phys. Rev. B **46**, 3391 (1992).
[56] J. A. C. Bland and C. A. F. Vaz, in *Ultrathin Magnetic Structures III*, edited by J. A. C. Bland and B. Heinrich (Springer-Verlag, Berlin, 2005), p. 233.

[57] A. Paoletti and L. Passari, Nuovo Cimento **32**, 25 (1964).
[58] V. Niculescu, K. Raj, T. J. Burch, and J. I. Budnick, Phys. Rev. B **13**, 3167 (1976).
[59] J. Moss and P. J. Brown, J. Phys. F: Met. Phys. **2**, 358 (1972). The value for the magnetic moment given in this reference is in very good agreement with our value. However, the authors do not mention the temperature at which the measurements were performed. We presume they were done at RT.
[60] C. M. Gürtler, Ph.D. thesis, University of Cambridge, 2001.
[61] M. Brockmann, M. Zölfl, S. Miethaner, and G. Bayreuther, J. Magn. Magn. Mater. **198**, 384 (1999).
[62] M. Goto and T. Kamimori, J. Phys. Soc. Jpn. **52**, 3710 (1983).
[63] J. A. C. Bland, S. J. Steinmüller, A. Hirohata, W. S. Cho, Y. B. Xu, C. M. Gürtler, G. Wastlbauer, A. Ionescu, T. Trypiniotis, and S. N. Holmes, J. Phys. D **36**, 2204 (2003).
[64] A. Hirohata, S. J. Steinmueller, W. S. Cho, Y. B. Xu, C. M. Guertler, G. Wastlbauer, J. A. C. Bland, and S. N. Holmes, Phys. Rev. B **66**, 035330 (2002).
[65] S. E. Andresen, S. J. Steinmuller, A. Ionescu, G. Wastlbauer, C. M. Guertler, and J. A. C. Bland, Phys. Rev. B **68**, 073303 (2003).
[66] L. J. van der Pauw, Philips Res. Rep. **13**, 1 (1958).
[67] Y. Nishino, S. Y. Inoue, S. Asano, and N. Kawamiya, Phys. Rev. B **48**, 13 607 (1993).
[68] S. M. Sze, *Physics of Semiconductor Devices*, 2nd ed. (Wiley, New York, 1981).
[69] I. I. Mazin, A. A. Golubov, and B. Nadgorny, J. Appl. Phys. **89**, 7576 (2001).
[70] Y. Bugoslavsky, Y. Miyoshi, S. K. Clowes, W. R. Branford, M. Lake, I. Brown, A. D. Caplin, and L. F. Cohen (unpublished).
[71] H. Xu, Y. G. Li, A. T. S. Wee, C. H. A. Huan, and E. S. Tok, Surf. Sci. **513**, 249 (2002).
[72] U. Starke, W. Meier, C. Rath, J. Schardt, W. Weiss, and K. Heinz, Surf. Sci. **377-379**, 539 (1997).
[73] H. Busse, J. Kandler, B. Eltester, K. Wandelt, G. R. Castro, J. J. Hinarejos, P. Segovia, J. Chrost, E. G. Michel, and R. Miranda, Surf. Sci. **381**, 133 (1997).
[74] U. Starke, J. Schardt, W. Weiss, W. Meier, C. Polop, P. L. D. Andres, and K. Heinz, Europhys. Lett. **56**, 822 (2001).
[75] S. J. Cowdery and F. X. Kayser, Mater. Res. Bull. **14**, 91 (1979).
[76] S. Pickart, T. Litrenta, T. Burch, and J. I. Budnick, Phys. Lett. **53A**, 321 (1975).